NASA CONTRACTOR REPORT

NASA CR-2400

NASA CR-2400

EDGE DIFFRACTED CAUSTIC FIELDS

by W. D. Burnside and L. Peters, Jr.

Prepared by

THE OHIO STATE UNIVERSITY

ELECTROSCIENCE LABORATORY

Columbus, Ohio 43212

for Langley Research Center

NATIONAL AERONAUTICS AND SPACE ADMINISTRATION • WASHINGTON, D. C. • MAY 1974

1. Report No.	2. Government Accession No.	3. Recipient's Catalog No.
NASA CR-2400		

4. Title and Subtitle	5. Report Date
EDGE DIFFRACTED CAUSTIC FIELDS	May 1974
	6. Performing Organization Code

7. Author(s)	8. Performing Organization Report No.
W. D. Burnside and L. Peters, Jr.	TR 2902-13
	10. Work Unit No. 502-33-13-02

9. Performing Organization Name and Address	11. Contract or Grant No.
The Ohio State University ElectroScience Laboratory Columbus, Ohio 43212	NGL 36-008-138
	13. Type of Report and Period Covered Contractor Report

12. Sponsoring Agency Name and Address	14. Sponsoring Agency Code
National Aeronautics and Space Administration Washington, D.C. 20546	

15. Supplementary Notes

Topical report.

16. Abstract

The fields near a caustic created by an edge diffraction process are computed using the equivalent current concept [1,2]. These fields are shown to have the property commonly associated with ray optical analysis or the Geometrical Theory of Diffraction (GTD), e.g., a 90° phase shift as the ray passes through the caustic. This result was predicted by Kay and Keller [3] on the basis of solutions for reflected fields from singly curved surfaces. The present effort is directed toward consideration of the caustic created by an edge diffraction process. Particular attention is focused on electromagnetic excitation. The acoustic excitation for the hard boundary condition is outlined in an appendix. In addition, our present goal is to establish the extent of the caustic region. This is of particular importance when a ray optical solution involves multiply-diffracted terms in that the minimum size of the body that can be analyzed may be restricted by the extent of the caustic, i.e., the 90° phase shift used in ray optical analysis may be introduced only if the caustic is contained on the surface being studied.

As a further application, these caustic fields would also prove useful in evaluating the surface current and charge density induced on a body in the shadow region. They would also provide the response of an elemental antenna placed in the shadow zone.

17. Key Words (Suggested by Author(s))	18. Distribution Statement
Antennas, Spacecraft and Aircraft Antennas Applied Electromagnetic Theory	Unclassified - Unlimited STAR Category 09

19. Security Classif. (of this report)	20. Security Classif. (of this page)	21. No. of Pages	22. Price*
Unclassified	Unclassified	32	$3.25

*For sale by the National Technical Information Service, Springfield, Virginia 22151

CONTENTS

EDGE DIFFRACTED CAUSTIC FIELDS

W. D. Burnside and L. Peters, Jr.

Introduction

The equivalent current concept has been applied implicitly in GTD solutions by various authors with Ryan and Rudduck[1,2] being among the earliest. It was formalized by Ryan and Peters[3,4] and applied to compute the radiation and scattered fields from a number of radiating systems. It has since been applied to obtain the complete radiation pattern from reflector antennas[5,6].

Senior and Uslengi criticized the equivalent current concept in a paper discussing the scattering of a cone[7]. Burnside and Peters[8] corrected the misleading impressions generated by Senior et.al. and included the equivalent current in treating the second order diffraction to improve the analysis of axial backscatter for a finite cone. The basis for the equivalent current concept is described compactly in our response to Senior's comments and it is repeated here. Following that discussion some new previously unpublished results obtained using the equivalent current technique are presented that in essence fixes the minimum size conducting body such as a cone that can be treated using the ray optical format.

Theoretical Background

Consider a two-dimensional wedge whose edge is y directed and lies at the coordinate origin ($r = 0$). The diffracted fields for a plane wave at normal incidence is given by

$$(1) \qquad u = \begin{Bmatrix} H_y^d \\ E_y^d \end{Bmatrix} = \{v_B(n,s,\phi^-) \pm v_B(n,s,\phi^+)\} \begin{Bmatrix} H_y^i \\ E_y^i \end{Bmatrix}$$

where the parameters are illustrated in Fig. 1 with

$$\phi^{\pm} = \psi \pm \psi_0 \ .$$

The incident and diffracted fields are given by

$$\begin{Bmatrix} H_y^i \\ E_y^i \end{Bmatrix}, \quad \begin{Bmatrix} H_y^d \\ E_y^d \end{Bmatrix}$$

respectively. For the observation point removed from the shadow boundaries and s sufficiently large

$$(2) \qquad v_B(n,r,\phi^{\pm}) \cong \frac{e^{-j\frac{\pi}{4}} e^{-jks}}{\sqrt{2\pi ks}} \left(\frac{1}{n} \sin\frac{\pi}{n}\right) \left(\frac{1}{\cos\frac{\pi}{n} - \cos\frac{\phi^{\pm}}{n}}\right) .$$

This form is used for all computations in this paper. Greater accuracy can be obtained for small values of s and for observation points much nearer the shadow boundary using a form given by Hutchins and Kouyoumjian[9]. Equation (2) can also be written in the form

$$(3) \qquad v_B(n,r,\phi^{\pm}) = \frac{e^{-j\frac{\pi}{4}} e^{-jks}}{\sqrt{4\pi ks}} G(n,\phi^{\pm}) .$$

It is seen that Equation (3) has the same range dependence as a line source.

The two dimensional fields of a y directed line current are given by

$$(4) \qquad E_y = - Z_o \, k \, I_y^e \left(\frac{e^{j\frac{\pi}{4}}}{2\sqrt{2\pi ks}}\right) e^{-jks}$$

for an electric line source with current I_y^e , and

$$(5) \qquad H_y = - Y_o \, k \, I_y^m \left(\frac{e^{j\frac{\pi}{4}}}{2\sqrt{2\pi ks}}\right) e^{-jks}$$

for a magnetic line source with current I_y^m as given by Harrington[10]. Equations (1) through (5) can be solved to give the equivalent currents [3],

$$(6) \qquad I_y^e = j \frac{2}{Z_o k} [G(n,\phi^-) - G(n,\phi^+)] \, E_y^i$$

and

$$(7) \qquad I_y^m = j \frac{2}{Y_o k} [G(n,\phi^-) + G(n,\phi^+)] \, H_y^i .$$

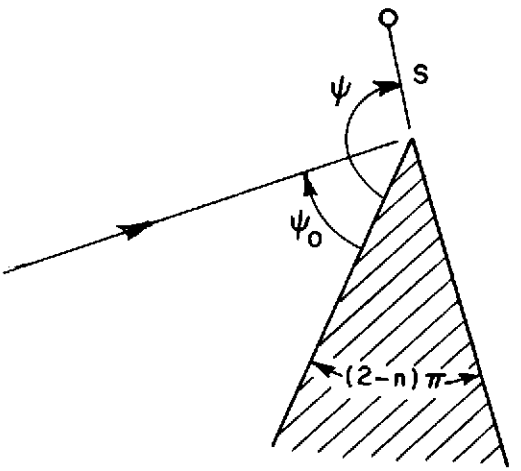

Fig. 1--Wedge Geometry

If the shape of the edge is distorted, then the diffracted fields are predicted from these currents, positioned in space to conform to the shape of the edge, in that diffraction is a localized phenomena.

The present study is restricted to the fields on the back surface or base of a cone (or disk) when a plane wave is axially incident on the cone as shown in Fig. 2. The Geometrical Theory of Diffraction (GTD) (or ray optical analysis) would predict that these rays are diffracted across the back through center of the base to the opposite side of disk. A 90° phase jump is introduced after the ray passes through the center. Since all rays converge at the center the ray optical analysis would predict that the fields at this point become infinite, and this represents the caustic region. These rays are then diffracted at the opposite edge of the cone base and are designated as second order diffracted rays. The ray that is launched in the direction of source contributes to the back scattered field[8]. It is the fields that exist on the base of the cone that are the subject of the present study. The GTD analysis yields

$$-E^{\theta} = E^{i} \sin\phi \sqrt{\frac{a}{r}}\, 2v_B\left(n,\ a\text{-}r,\ \frac{3\pi}{2}\right)$$

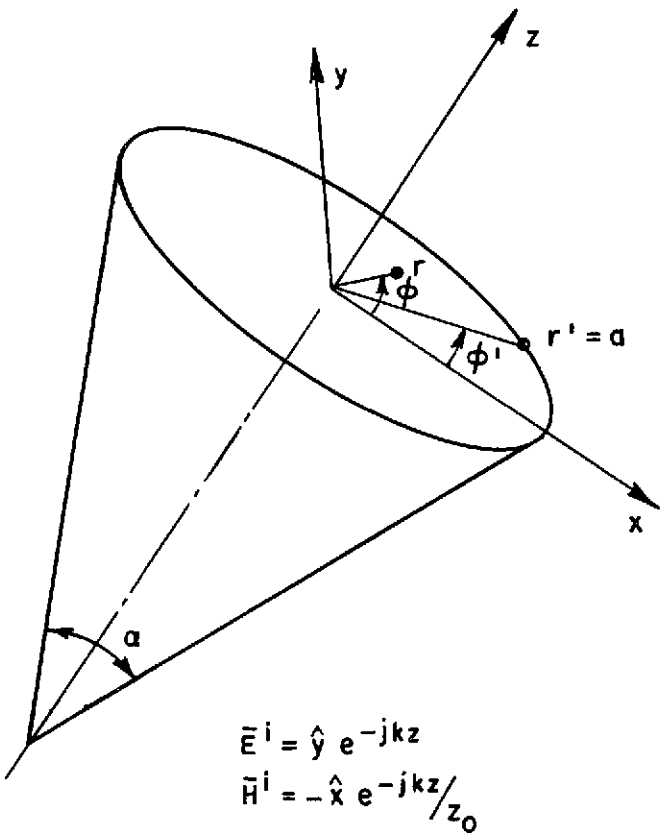

Fig. 2--Cone Geometry

for $0 < \phi < \pi$ and $0 < \phi' < \pi$

or $\pi < \phi < 2\pi$ and $\pi < \phi' < 2\pi$

and

$$-E^{\theta} = -E^{i} \sin\phi \sqrt{\frac{a}{r}}\, 2v_B\left(n,\ a+r,\ \frac{3\pi}{2}\right) e^{j\frac{\pi}{2}}$$

for $\pi < \phi' < 2\pi$ and $0 < \phi < \pi$

or $0 < \phi' < \pi$ and $\pi < \phi < 2\pi$

It is the $\sqrt{\frac{a}{r}}$ factor that causes the GTD result to approach infinity as $r \to 0$. The $\sin\phi$ factor is introduced by the polarization of the incident wave. It would not be present in the acoustical case for the hard boundary condition.

The equivalent currents have been introduced for the express purpose of obtaining the correct value of the fields in the vicinity of the caustic.

The value of I^e, given by Equation (6), required to compute fields on the surface of the conducting wedge is identically zero. Thus only I^m is used in this paper since our interest is focussed primarily on the fields at the surface. Similarly for the acoustic case, only the hard boundary condition is considered.

The field configuration of interest is that of the normal electric field in the vicinity of the caustic on the surface of a perfectly conducting body with a wedge type of discontinuity. A circular geometry is considered since it can be done analytically and the essential features of the caustic region can be established. This circular geometry could be used directly for studies of both cones and disks. For plane wave incidence along the axis of symmetry, the caustic would exist in the vicinity of $r = 0$. Our attention is further restricted to the surface at the base of the cone corresponding to $z = 0$. The incident field is specified by

$$\overline{E}^{i} = \hat{y}\, e^{-jkz}$$

$$\overline{H}^{i} = -\hat{x}\, \frac{e^{-jkz}}{Z_o}$$

Analysis

The equivalent current at the rim of a cone or disk (at r = a) is of interest and is given by

$$I_{\phi}^{m} = \frac{j2}{k}\left[G(n,\phi^{-}) + G(n,\phi^{+})\right] (-\sin\ \phi)$$

$$= \frac{j4}{k} G\left(n, \frac{3\pi}{2}\right) (-\sin\ \phi') \tag{8}$$

for the geometry shown in Fig. 2. The z component of the electric field at the surface is given by

$$E_z = \frac{jka}{4\pi} \int_0^{2\pi} I_{\phi}^{m} \frac{e^{-jk|\bar{r}-\bar{r}'|}}{|\bar{r}-\bar{r}'|}\, d\phi' \tag{9a}$$

It is most important to note that Equation (9) is valid only in the vicinity of the caustic. The current I_{ϕ}^{m} is not an actual current but is only an equivalent current and is a valid representation only in the direction of the diffracted rays. Equation (9) will yield accurate results in the general vicinity of the caustic or for r small for our geometry. The equivalent currents are based on the concepts of edge diffraction and it represents a valid approach only in the vicinity of a converging ray bundle. It would yield approximate results for other values of r as long as a diffracted ray exists at that point, since this would represent a dominant term which would be obtained from Equation (9) via a stationary phase process. Balanis[13]has used the stationary phase concept to properly evaluate the fields caused by an edge diffraction process. However, Equation (9a) cannot be used in general to evaluate a low level field at a point far removed from the caustic where there is no propagating ray. To the extent that Equation (9a) yields a result that deviates from the ray optical solution for an observation point far removed from the caustic, it is in error. The limits of integration of Equation (9) give the total electric field on the base of the cone. This will set up a standing wave pattern since the currents for $0 < \phi' < \pi$ will launch a set of diffracted fields as will the currents for $\pi < \phi' < 2\pi$. These two sets of diffracted fields will interact and create a standing wave pattern which will obscure the caustic field structure. If the integration limits are $0 < \phi' < \pi$, only a single set of caustic fields are computed and no standing wave pattern appears. Most of the results presented in this paper are based on this range of integration so that the interference pattern is not included or

$$E_z = \frac{jka}{4\pi} \int_0^{\pi} I_{\phi}^{m} \frac{e^{-jk|\bar{r}-\bar{r}'|}}{|\bar{r}-\bar{r}'|}\, d\phi' \ . \tag{9b}$$

Approximate Form of Caustic Fields

It is instructive to examine the characteristics of the caustic on a functional basis to obtain a further understanding of its form and extent and also to extract the phase jump introduced as a ray propagates through the caustic region.

For observation points on the surface, the approximations

$$\frac{1}{|\bar{r}-\bar{r}'|} = \frac{1}{a} \tag{10}$$

and

$$k|\bar{r}-\bar{r}'| = k\sqrt{a^2 + r^2 - 2ar\cos(\phi-\phi')} \tag{11}$$

$$\approx k\left(a + \frac{1}{2}\frac{r^2}{a} - r\cos(\phi-\phi')\right) \tag{12}$$

are made for $r << a$. Thus

$$-E_\theta = E_z = A\int_0^{2\pi} \sin\phi' \, e^{jkr\cos(\phi-\phi')}\, d\phi' \tag{13}$$

where

$$A = \frac{1}{\pi} e^{-jk\left(a + \frac{1}{2}\frac{r^2}{a}\right)} G\left(n, \frac{3\pi}{2}\right)$$

By use of the relation

$$e^{jkr\cos(\phi-\phi')} = \sum_{n=-\infty}^{\infty} j^n J_n(kr)\, e^{jn(\phi-\phi')}\,, \tag{14}$$

$$-E_\theta = E_z \approx 2j\sin\phi\, J_1(kr)\, e^{-jk\left(a+\frac{1}{2}\frac{r^2}{a}\right)} G\left(n, \frac{3\pi}{2}\right) \tag{15}$$

The fields removed from the surface would be obtained using essentially the same procedure but would require a contribution of the equivalent electric current of Equation (6). The approximation of Equation (12) is accurate within 10% provided $r/a < 0.2$ as is easily shown by means of the binomial expansion. However, this may not prove adequate in the phase term and in fact for $a/\lambda = 10$, r must be less than λ in order that the phase error introduced by this approximation be less than 20°. On the other hand, for $a/\lambda = 1.0$ and $r = 0.2$ the maximum phase error is less than 10°.

Another basic limitation exists in that the equivalent current representation which is based on the asymptotic form of the diffraction coefficient requires $ks\,(1 + \cos\phi^{\pm}) >> 1$. This condition is well satisfied provided $s > \lambda/2$ except near the shadow boundaries ($\phi^{\pm} = \pi$). This possibility does not occur here.

The factor $J_1(kr)$ has a maximum at $kr = 1.8$ and a minimum at $kr = 3.8$ corresponding to $r/\lambda = .27$ and 0.61, respectively. Later it is demonstrated that the two point diffraction mechanism is all that is required to properly evaluate the fields for $r/\lambda > 1/2$ which corresponds closely to the first minimum of $J_1(kr)$. For $r/\lambda > 1/2$, the observation point then is outside the caustic region.

Equation (15) could be obtained from the GTD analysis provided one uses the asymptotic form of

$$J_1(kr) \sim \sqrt{\frac{2}{\pi kr}} \cos\left(kr - \frac{3\pi}{4}\right)$$

The GTD solution has the form

$$-E_\theta = \sqrt{\frac{a}{r}} \sin\phi \left\{ 2v_B\left(n, a-r, \frac{3\pi}{2}\right) - 2v_B\left(n, a+r, \frac{3\pi}{2}\right) e^{j\frac{\pi}{2}} \right\}$$

$$= \sqrt{\frac{a}{r}} \sin\phi \, \frac{2G\left(n, \frac{3\pi}{2}\right)}{\sqrt{2\pi ka}} e^{-jka} \left\{ e^{j\left(kr - \frac{\pi}{4}\right)} + e^{-j\left(kr - \frac{5\pi}{4}\right)} \right\}$$

$$= \frac{2 \sin\phi}{\sqrt{2\pi kr}} G\left(n, \frac{3\pi}{2}\right) j e^{-jka} \left\{ e^{j\left(kr - \frac{3\pi}{4}\right)} + e^{-j\left(kr - \frac{3\pi}{4}\right)} \right\}$$

$$= 2j \sin\phi \, G\left(n, \frac{3\pi}{2}\right) e^{-jka} \left\{ \sqrt{\frac{2}{\pi kr}} \cos\left(kr - \frac{3\pi}{4}\right) \right\}$$

which can now be related to Equation (15).

Charge and Current Densities

The magnetic field intensity at the suface of the conductor, is given by

$$\overline{H} = -\frac{1}{j\omega\mu} \nabla \times \overline{E}$$

Normal $\overline{H}$ is identically zero over the conducting surface, so $H_\theta|_{\theta=90°} = 0$. Thus

$$\bar{H}\Big|_{\theta=90^\circ} = -\frac{1}{j\omega\mu}\left\{\hat{r}\,\frac{1}{r}\left[\frac{\partial E_\phi}{\partial\theta} - \frac{\partial E_\theta}{\partial\phi}\right] + \hat{\phi}\,\frac{1}{r}\left[r\,\frac{\partial E_\theta}{\partial r} + E_\theta - \frac{\partial E_r}{\partial\theta}\right]\right\}$$

It would appear that we must now evaluate the additional components of the electric field intensity. However, these can be approximated rather accurately using the terms that have already been obtained. First, note that the equivalent electric currents need not be introduced since they would produce only a magnetic field perpendicular to the conducting surface at $\theta = 90°$. Second, E_z and H_ϕ are related for a single ray by the intrinsic impedance of free space in the region where the ray optical computations are valid such that $E_z = \pm Z_o H_\phi$. This includes only a single ray propagating in one direction only and the sign is fixed by the direction of propagation. If there are two rays, H_ϕ is computed independently for each case and the total magnetic field intensity is, then, the vector sum of two terms. Finally in the vicinity of the caustic, under the condition that $r \ll a$,

$$E_\phi \approx 0$$

$$E_r = E_z \cos\theta$$

$$E_\theta \approx -E_z \sin\theta$$

where E_z is given by Equation (13). With these approximations, the magnetic field intensity at the surface is given by

$$\bar{H}\Big|_{\theta=90^\circ} = -\frac{1}{j\omega\mu}\left\{-\hat{r}\,\frac{\partial E_\theta}{\partial\phi} + \hat{\phi}\,\frac{\partial E_\theta}{\partial r}\right\}$$

or

$$\bar{H}\Big|_{\theta=90^\circ} = \frac{2e^{-jk\left(a+\frac{1}{2}\frac{r^2}{a}\right)}}{\omega\mu r}\, G\left(n, \frac{3\pi}{2}\right)\left\{\hat{r}\cos\phi\, J_1(kr)\right.$$

$$+ \hat{\phi}\sin\phi\left(k\left[J_o(kr) - \frac{1}{kr}J_1(kr)\right]\right.$$

$$\left.\left. - \frac{jkr}{a}J_1(kr)\right)\right\} \qquad (16)$$

Equations (15) and (16) may be used to evaluate the surface charge and current densities, respectively. The surface charge density is given by

$$\rho = \varepsilon_o\, \hat{n} \cdot \bar{E}$$

or

$$\rho = 2\varepsilon_0 j\, J_1(kr) \sin\phi\, e^{-jk(a + \frac{1}{2}\frac{r^2}{a})}\, G\left(n, \frac{3\pi}{2}\right)$$

The surface current density ($\overline{J} = \hat{n} \times \overline{H}$)is also readily obtained using Equation (16).

Caustic Fields for Half Rim Excitation

To obtain the field structure when only the rim for $0 < \phi' < \pi$ is excited, Equation (9b) was formulated. Now Equation (13) becomes

$$-E_\theta = E_z = A \int_0^\pi \sin\phi'\, e^{jkr\cos(\phi - \phi')}\, d\phi' \tag{17}$$

where

$$A = \frac{1}{\pi} e^{-jk(a + \frac{1}{2}\frac{r^2}{a})}\, G(n, \tfrac{3\pi}{2})$$

Again making use of Equation (14),

$$-E_\theta = A \sum_{-\infty}^{\infty} e^{jn\phi}\, j^n J_n(kr) \int_0^\pi \sin\phi'\, e^{-jn\phi'}\, d\phi'$$

After some manipulation, this reduces to

$$-E_\theta = A\left\{2J_0(kr) + j\pi J_1(kr)\sin\phi + \sum_{n=1}^{\infty} \frac{2J_{2n}(kr)}{1-(2n)^2}\, 2\cos 2n(\phi + \tfrac{\pi}{2})\right\} \tag{18}$$

The asymptotic form of the Bessel functions are

$$J_{2n}(kr) = \sqrt{\frac{2}{\pi kr}}\cos\left(kr - \frac{\pi}{4} - \frac{2n\pi}{2}\right) \tag{19}$$

$$= \sqrt{\frac{2}{\pi kr}}\cos\left(kr - \frac{\pi}{4}\right)\cos n\pi$$

and recognizing the series[11]as given by

$$S = \sum_{1}^{\infty} \frac{\cos 2n\phi}{n^2 - 1} = 2 - \pi\sin\phi \tag{20}$$

plus the fact that

$$S(\phi) = S(\pi + \phi) \tag{21}$$

for $0 < \phi < \pi$. These results are used to cast Equation (18) into the form

$$-E_\theta = A\sqrt{\frac{2}{\pi kr}}\,\pi \sin\phi\, e^{j\left(kr - \frac{\pi}{4}\right)} \tag{22}$$

$$\text{for } 0 \leq \phi \leq \pi$$

and

$$-E_\theta = A\sqrt{\frac{2}{\pi kr}}\,\pi \sin\phi\, e^{-j\left(kr - \frac{5\pi}{4}\right)} \tag{23}$$

$$\text{for } \pi \leq \phi \leq 2\pi$$

This last step would apparently introduce an additional phase shift of $-\pi/2$ radians as the wave propagates through the caustic. However, the $\sin\phi$ factor reverses sign and makes this $+\pi/2$ radian phase shift which is in agreement with the previously accepted result. Note that Equations (22) and (23) contain all of the restrictions implicit in Equation (17).

Straightforward application of ray optical techniques would give for distances removed from the caustic

$$-E_\theta = G\left(n, \frac{3\pi}{2}\right) e^{-j\left[k(a-r)+\frac{\pi}{4}\right]} \frac{1}{\sqrt{2\pi k(a-r)}} \sqrt{\frac{a}{r}} \sin\phi$$

$$\text{for } 0 \leq \phi \leq \pi$$

and

$$-E_\theta = -jG\left(n, \frac{3\pi}{2}\right) e^{-j\left[k(a+r)+\frac{\pi}{4}\right]} \frac{1}{\sqrt{2\pi k(a+r)}} \sqrt{\frac{a}{r}} \sin\phi$$

$$\text{for } \pi < \phi < 2\pi\ .$$

Comparing these equations with Equations (22) and (23) shows that the assumed phase jump has indeed been introduced after the ray passes through the caustic region.

Expressions for Fields at the Rim

To date our attention has been focussed on the fields in the vicinity of the caustic. Let us now consider the fields at the rim of the disk. The excitation is again restricted to $0 < \phi' < \pi$ and the observation point is now placed at $r = a$ and $\pi < \phi < 2\pi$. The range dependence is given by

$$|\bar{r} - \bar{r}'| = \sqrt{a^2 + r^2 - 2ar\cos(\phi-\phi')}$$

$$= 2a \sin \frac{\phi - \phi'}{2}$$

It is again noted that Equation (9) is a valid representation only in the vicinity of the caustic. Any expression for the fields at the rim of the cone base can be considered to be valid only when the fields are large. Such an expression is formulated and evaluated at one point on the rim. It is used to indicate of the extent of the caustic fields. The integral has the form

$$(24) \qquad -E_\theta = E_z = \frac{G\left(n, \frac{3\pi}{2}\right)}{2\pi} \int_0^\pi \frac{\sin\phi' \, e^{j2ka \sin \frac{(\phi-\phi')}{2}}}{\sin \frac{\phi - \phi'}{2}} d\phi'$$

The integral remains finite at the edge because of the restrictions placed on ϕ, ϕ'. Equation (9b) has been evaluated numerically for $r = a$, corresponding to observation points on the rim of the cone base. The results are to be discussed later.

Equation (24) can be evaluated analytically for the specific value of $\phi = \pi$. This point occurs at the position where ray optics would predict a field strength of 0. The solution of Equation (24) at $\phi = \pi$ is

$$(25) \qquad -E_\theta = \frac{G\left(n, \frac{3\pi}{2}\right)}{2\pi} e^{jka} \left(\frac{4 \sin ka}{ka}\right)$$

Equation (25) has its first null at $ka = \pi$ corresponding to $a/\lambda = 1/2$ This is considered to be the extent of the caustic region, i.e. when the base radius $a/\lambda < 1/2$, the caustic covers the complete base of the cone, at least in the $\phi = \pi$ plane. At this stage, the postulate is made that the ray optics formulation is valid for $a > \lambda/2$. Note that Equation (25) is not accurate for $a/\lambda > 1/2$.

Results

The results obtained using Equation (9a) and (9b) with $a/\lambda = 10$ for $x = z = 0$ are compared with those obtained using conventional ray optical or GTD techniques in Fig. 3 and 4. Use of these equations eliminate the approximations made in the integration but those inherent in the equivalent current concept remain. The amplitude results show reasonable agreement when y is in excess of 0.2λ for both the case where the entire rim of the base of the cone is illuminated (Fig. 3a) and also where only half the rim is illuminated (Fig. 3b). In these curves, the ray has passed through the caustic for negative values of y. Similar conclusions can be drawn for the phase of the fields in the vicinity of the caustic from Fig. 4. The effect of the propagation path has been removed in the phase plot of Fig. 5 to more clearly illustrate the caustic phase shift. This curve is offset by $-45°$ before the caustic because of the $e^{-j\,\pi/4}$ factor in the diffraction coefficient of Equation (2). It would appear that the ray optical assumption of a 90° phase shift is essentially correct for $y/\lambda > 0.5$. This compares favorably to the value of $a/\lambda > 1/2$ obtained in the preceding section pertaining to the base radius at which the caustic region covered the cone base.

The conclusions thus have been made from results obtained using a cone with a 10λ base radius. In the following paragraphs, the effects of the base radius are to be evaluated.

Equation (18) indicates that the amplitude of the caustic is independent of the base radius provided the assumptions made in its derivation are valid. Fig. 6 shows the amplitude curves of the normal E field for different cone base radii as obtained from Equation (9b). There is some dependence on the base radii but within the values of r, a and λ for which Equation (18) is valid this is a rather small variation, and indeed at $r = 0$, the magnitude $|E_z| = .45$ for all values of a. The black dots indicate the GTD solution. Note that the GTD solution is valid outside the regions illustrated in Fig. 6.

The phase variations through the caustic region for different base radii are shown in Fig. 7. The 90° phase jump of the ray optical solution is not achieved for smaller base radii. For $a/\lambda > 0.5$, $\phi = 180$, a phase error less than 25° is made when the 90° phase jump is used. These results would be useful in the evaluation of charge density on the base of the cone or for computing the voltage at the terminals of an antenna element placed on the cone.

In order to compute the back scattered fields of the cone, one must know the fields at the opposite rim of the cone. These have been computed using Equation (9b). As we have ascertained, the phase is the most significant parameter and it is shown in Fig. 8. The phase jump caused by passing through the caustic region is significantly different than the 90° phase jump of GTD for smaller radii bases. For $a/\lambda = 0.5$ a phase error of 20° is introduced when the 90° phase jump is introduced according to the ray optical analysis. Fig. 6 would indicate that the

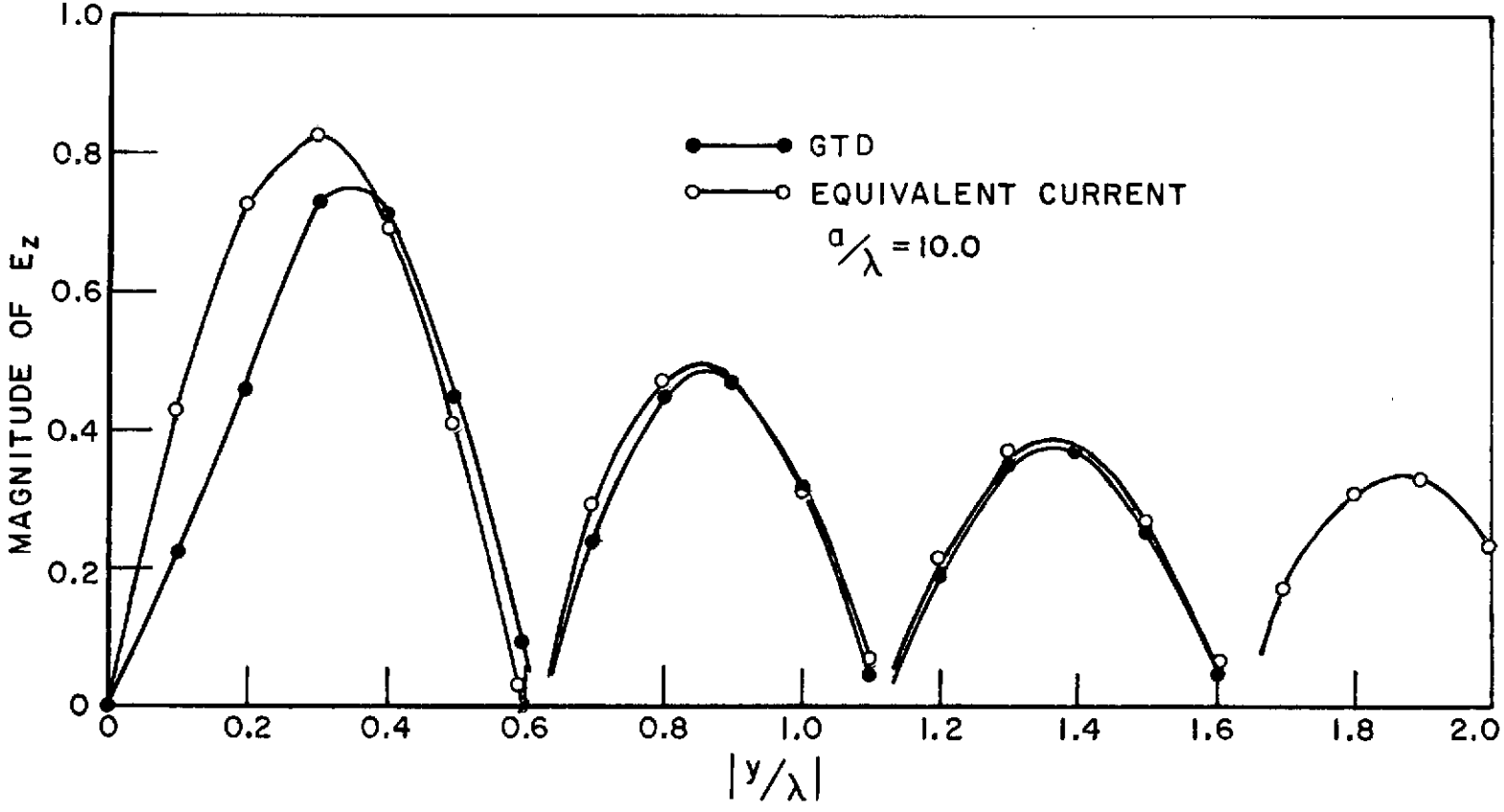

Fig. 3--Magnitude of E_z in Caustic Region
a) for Complete Rim Excitation $0 < \phi' < 2\pi$

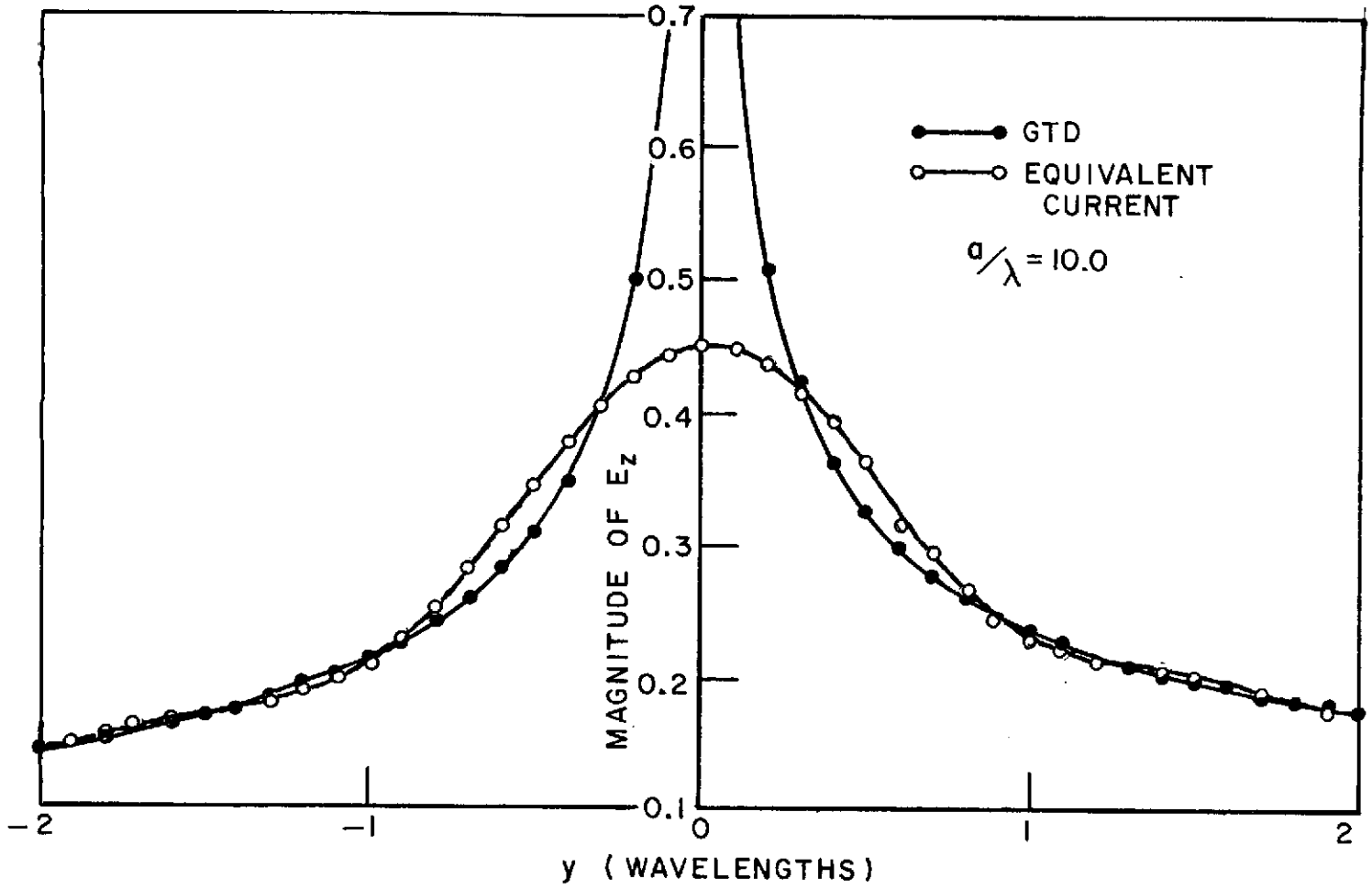

Fig. 3--Magnitude of E_z in Caustic Region
b) for Half Rim Excitation $0 < \phi' < \pi$

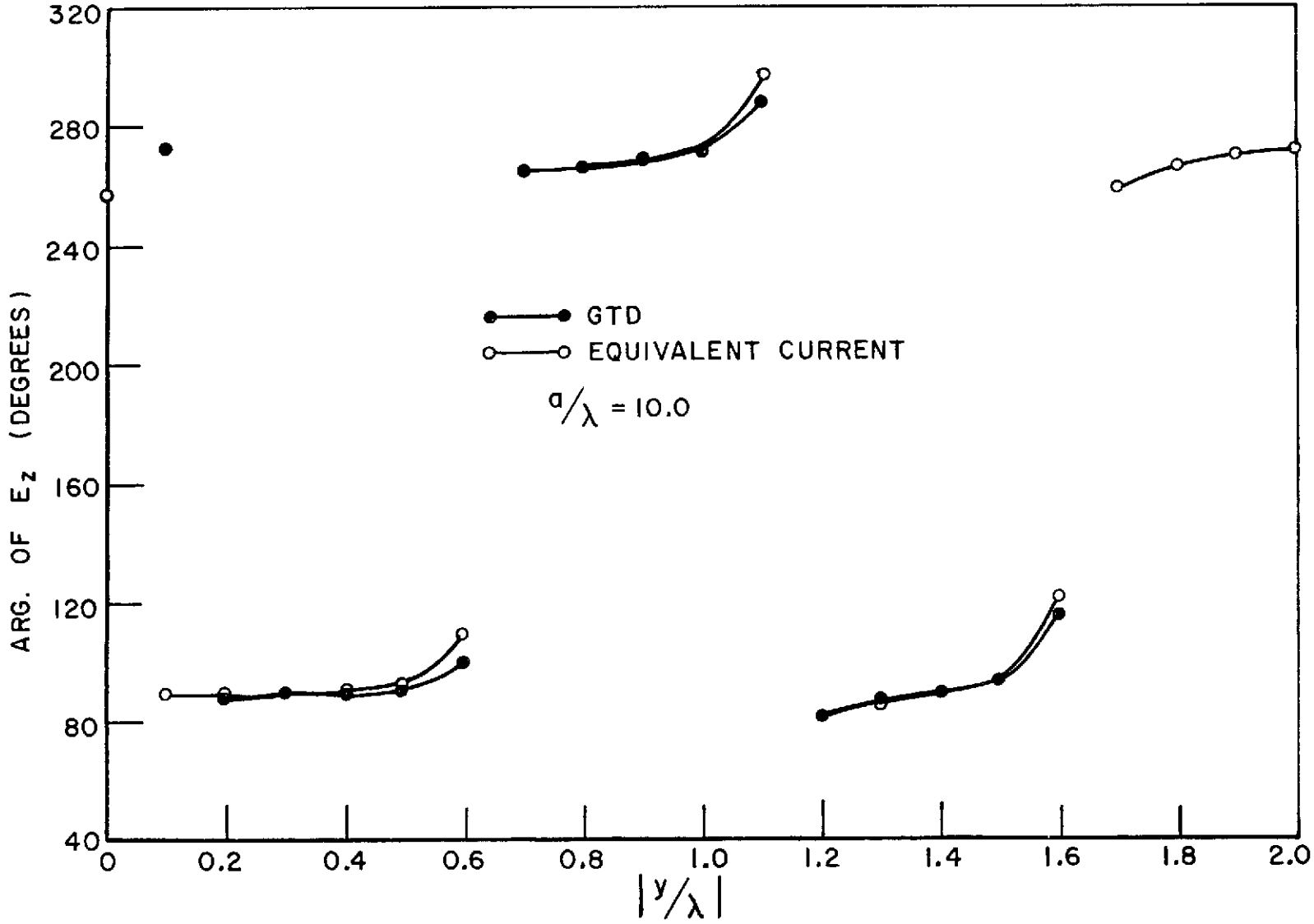

Fig. 4--Argument of E_z in Caustic Region
a) for Complete Rim Excitation

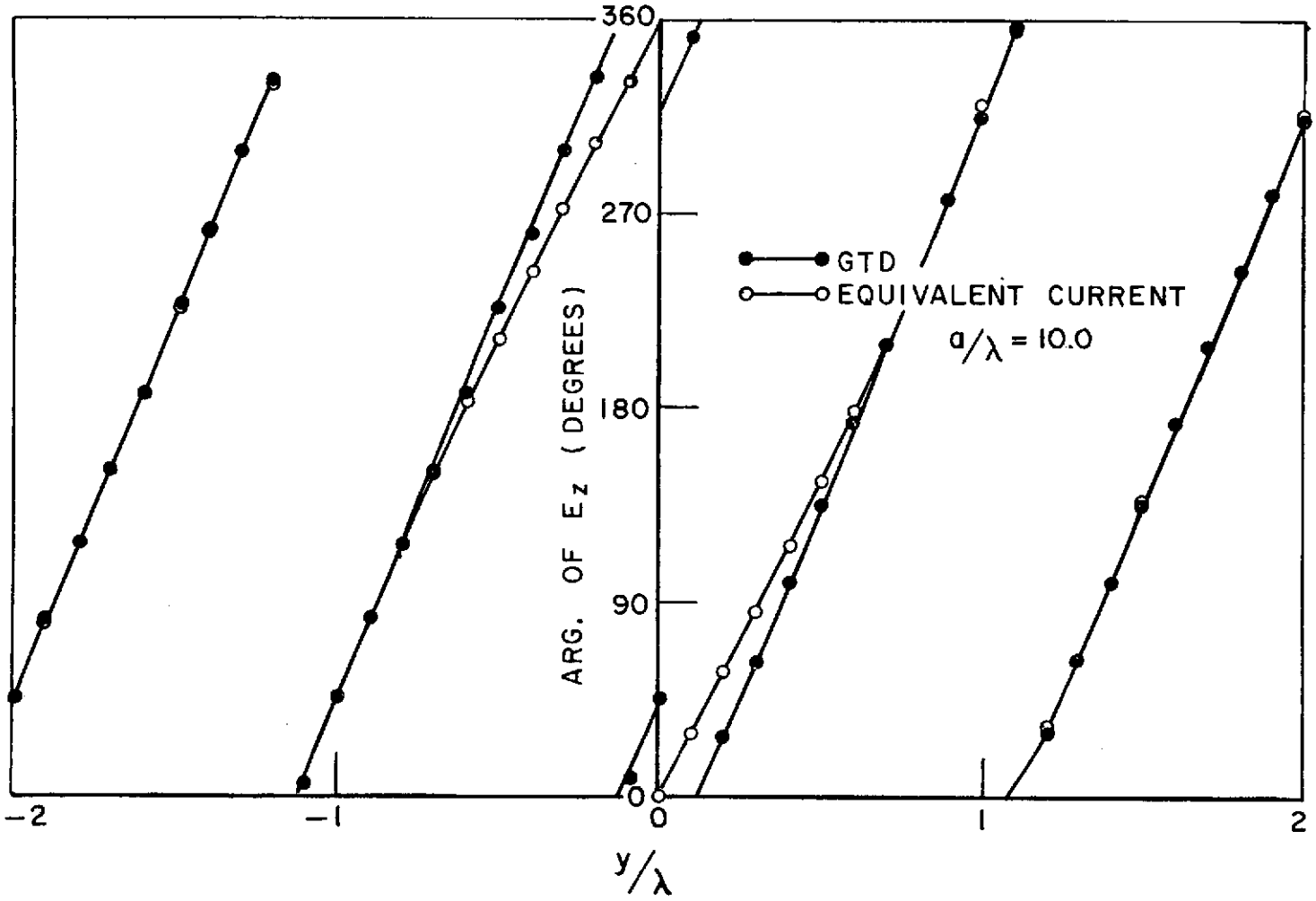

Fig. 4--Argument of E_z in Caustic Region
b) for Half Rim Excitation

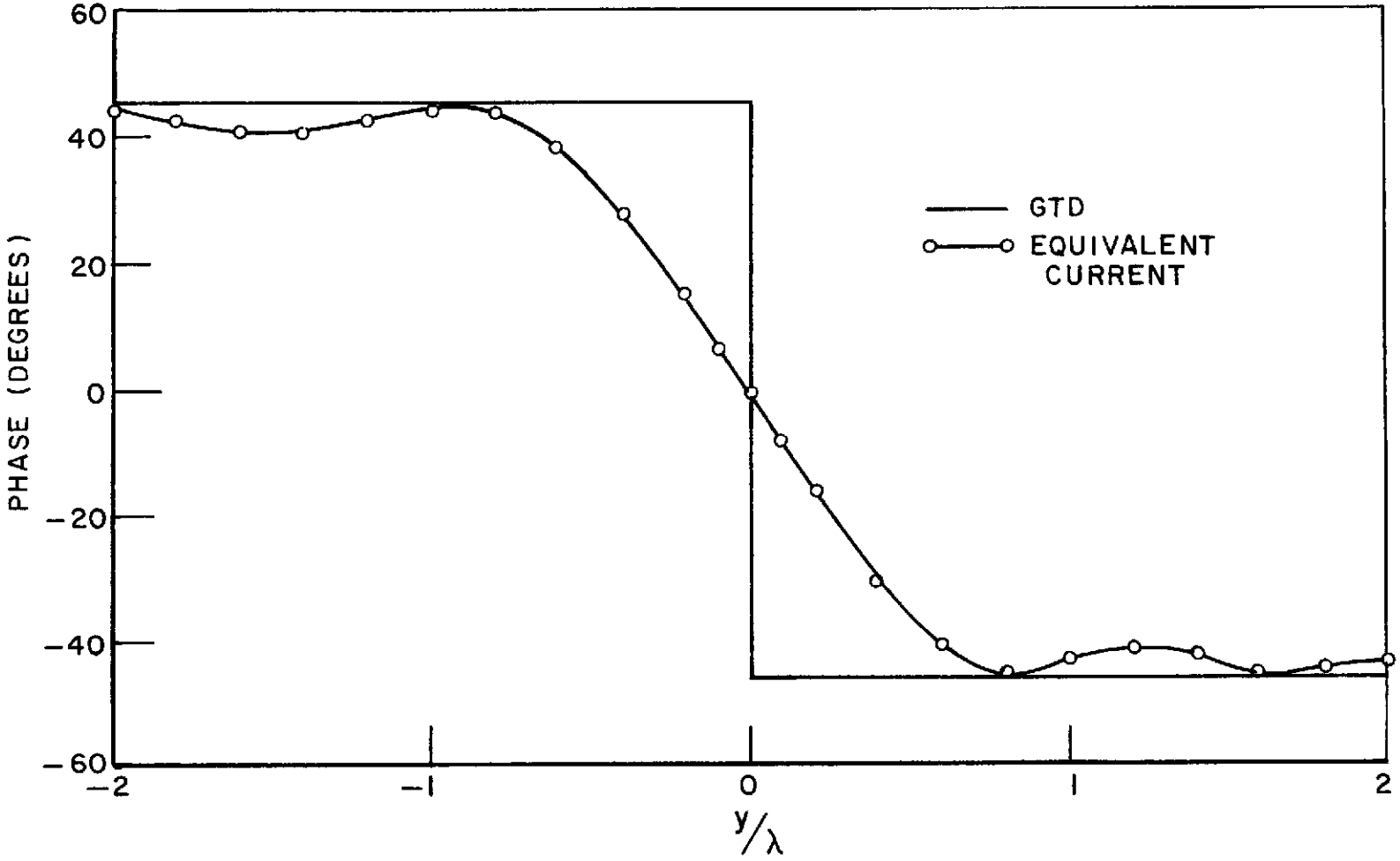

Fig. 5--Argument of E_z in Caustic Region with Propagation Phase Shift Removed

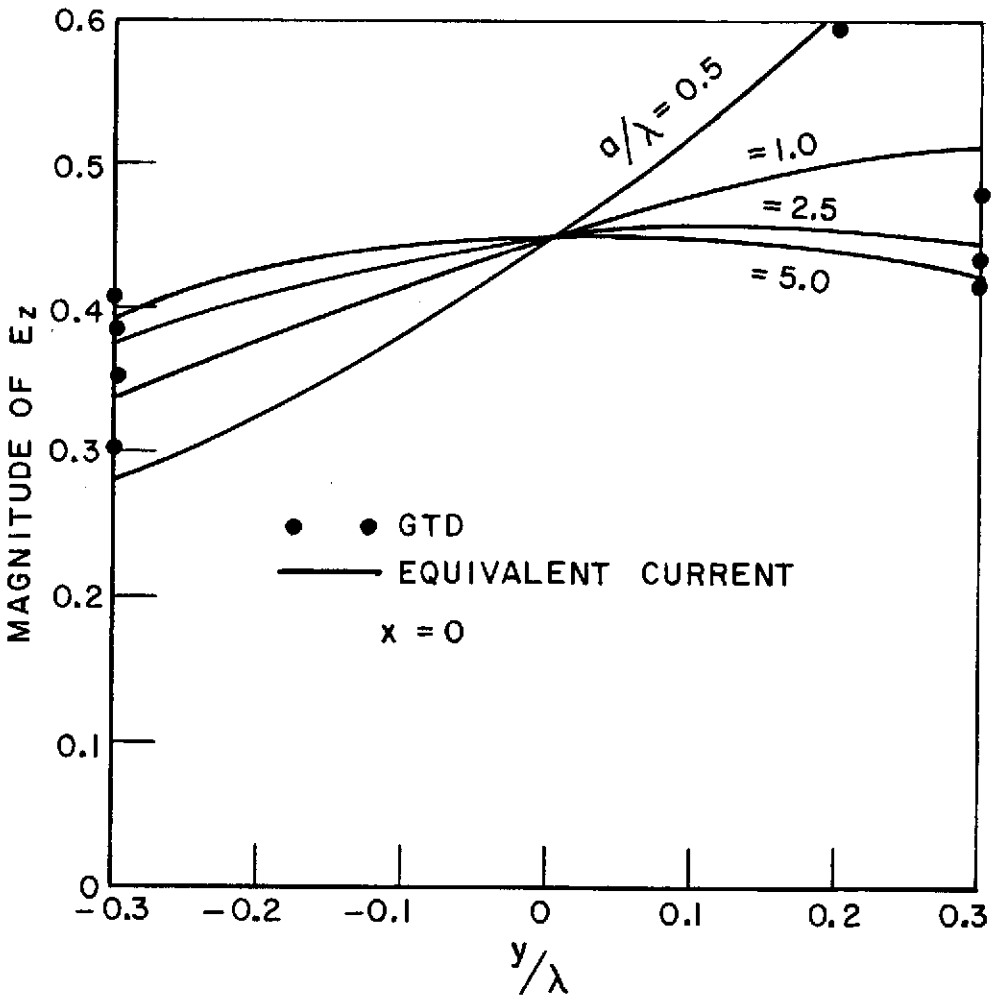

Fig. 6--Magnitude of E_z in Caustic Region for Different Cone Base Radii

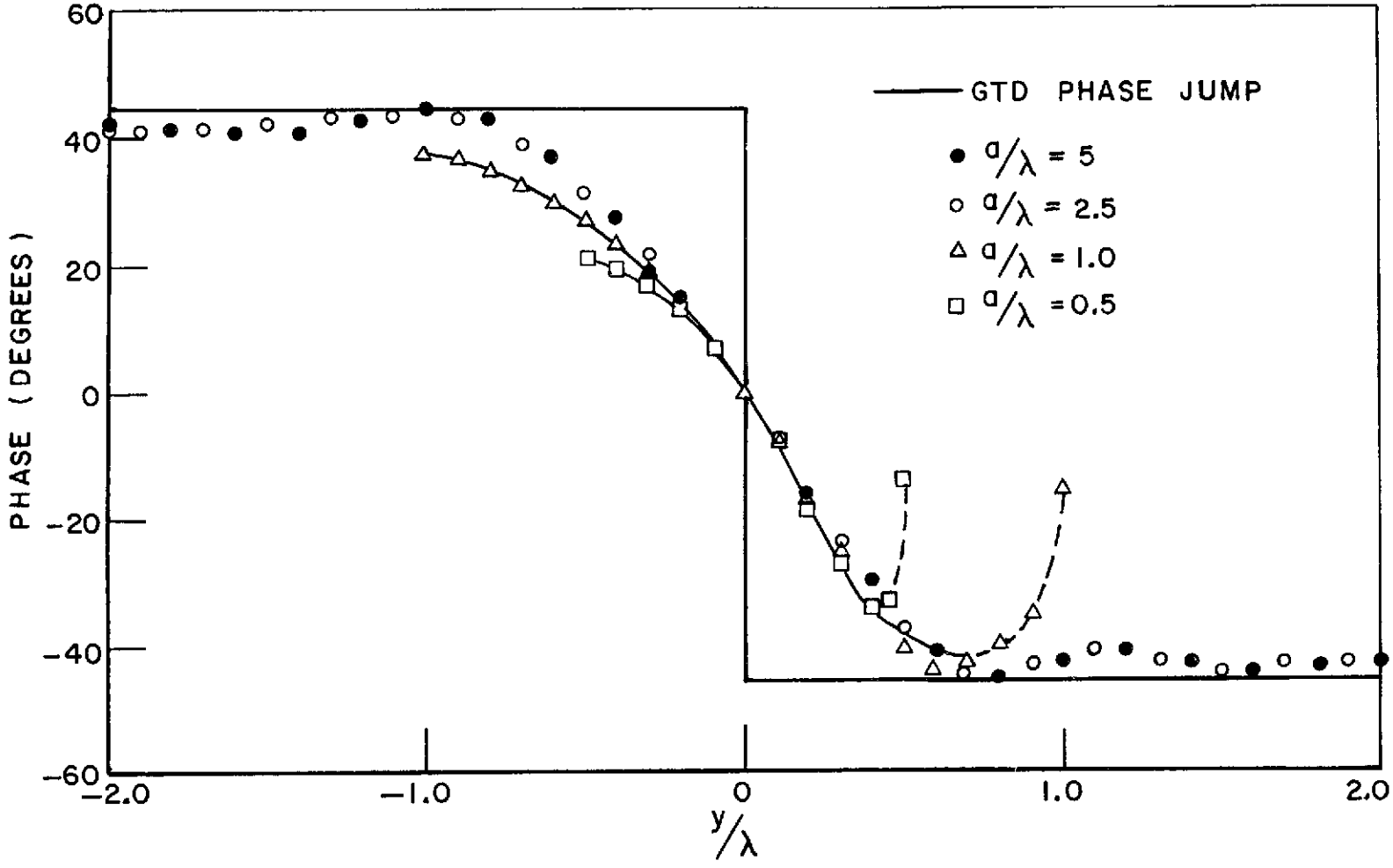

Fig. 7--Argument of E_z in Caustic Region with Propagation Phase Shift Removed for Different Cone Base Radii

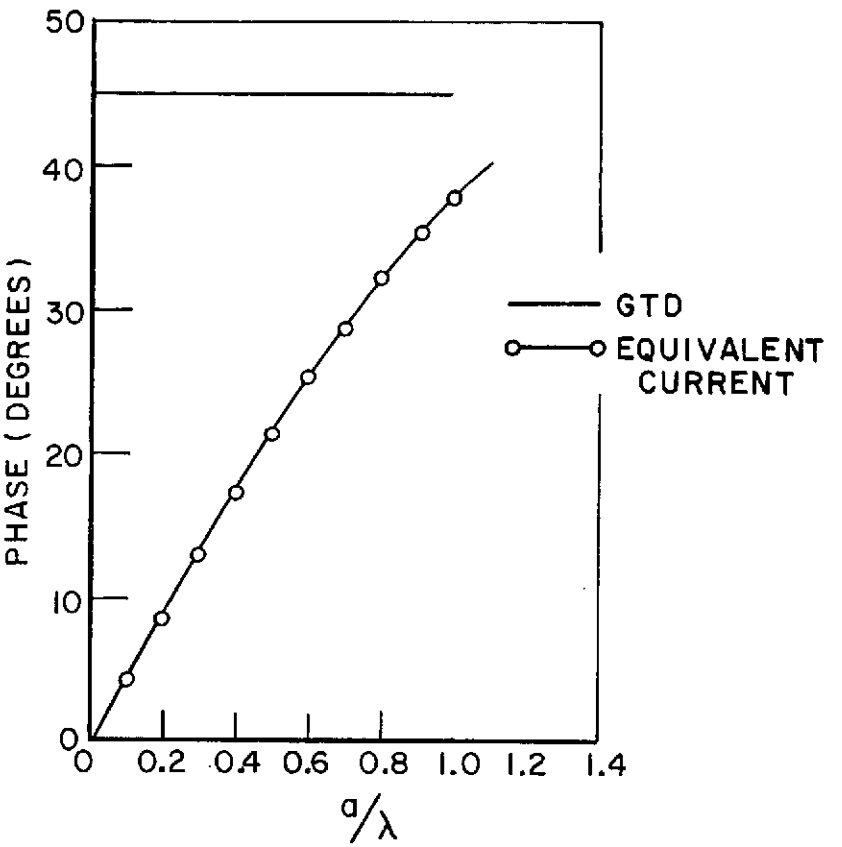

Fig. 8--Phase at Rim with Propagation Phase Shift Removed

correct magnitude is predicted by GTD for r/λ as small as 0.2. However, this indication seems to be valid only for observation points near $\phi = 270°$.

It has been noted earlier that the caustic introduces a significant perturbation from the fields computed by GTD at the rim when $a/\lambda < 1/2$. This has been verified again using Equation (9b) for $a/\lambda = 1/2$, 1, 2.5 and 5.0 as a function of ϕ when $\pi < \phi < 2\pi$. As predicted previously the fields at $\phi = \pi$ are negligibly small. The GTD analysis would predict the magnitude at the rim to be $A(\phi) = A(\phi = 270) \sin \phi$. This assumption has been observed to be valid for

$$\text{no } \phi \qquad (a/\lambda = 0.25)$$

$$210° < \phi < 330° \quad (a/\lambda = 1/2)$$

$$204° < \phi < 336° \quad (a/\lambda = 1)$$

$$200° < \phi < 340° \quad (a/\lambda = 2.5)$$

$$188° < \phi < 352° \quad (a/\lambda = 5.0)$$

The phase term is usually the term in which the error is first observed and the expected phase shift (that of Fig. 8) is obtained for

$$252° < \phi < 288° \quad (a/\lambda = 1/2)$$

$$210° < \phi < 330° \quad a/\lambda = 1$$

$$206° < \phi < 334° \quad a/\lambda = 2.5$$

$$200° < \phi < 340° \quad a/\lambda = 5.0$$

It has been previously postulated that the extent of the caustic region is essentially $r \leq 0.5\lambda$. Yet it has been shown that the conventional ray optical solution produces a reasonable amplitude along the $x = 0$ axis for $r \geq 0.2\lambda$. In order to resolve this question, the fields were computed at $r = a$, $\pi < \phi < 2\pi$ (on the rim) for $a = \lambda/4$. It was not too surprising to find that the amplitude did not follow the $A(\phi) = A(\phi = 270°) \sin \phi$ formula but were nearly constant ranging from 0.235 at $\phi = 270°$ to 0.287 at $\phi = 180$ and 360°. This merely indicates that the observation point is now in the caustic region over the entire base as has been suggested previously even though the GTD analysis predicts the correct amplitude at $x = 0$, $y = a$. Thus the fields are no longer local in nature and GTD does not give precise results for this small a cone base radius.

Finally, contour plots of the magnitude of normal E at the base of the cone are shown in Figs. 9 and 10 as obtained from Equation (9a) and (9b), respectively. The standing wave pattern shown in Fig. 9 is caused by waves being launched at opposite sides of the base of the cone masks the shape of the caustic field. The caustic field region is more

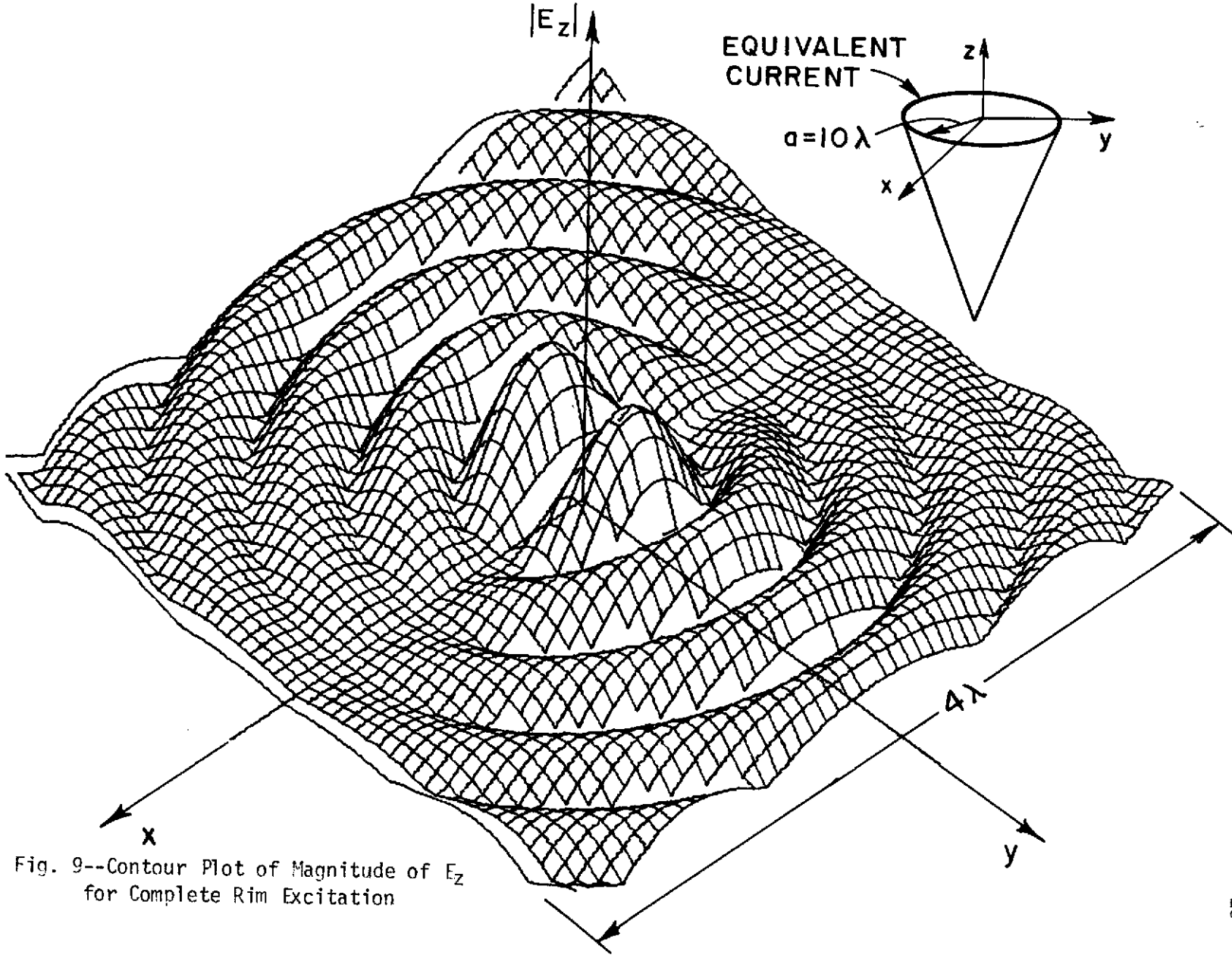

Fig. 9--Contour Plot of Magnitude of E_z for Complete Rim Excitation

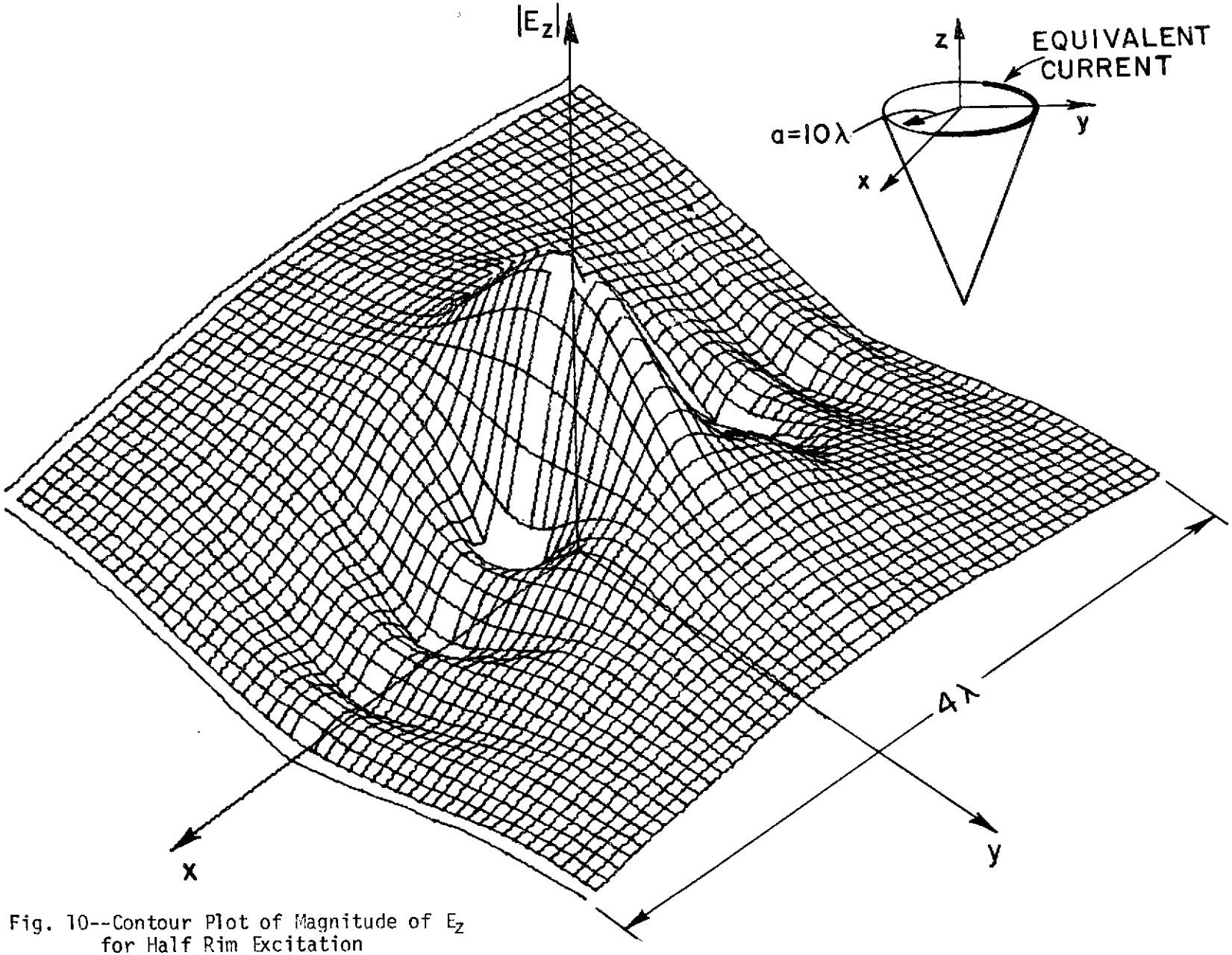

Fig. 10--Contour Plot of Magnitude of E_z for Half Rim Excitation

clearly seen in Fig. 10 where only the currents for $y > 0$ are included. The ripple observed in $y = 0$ plane is in this case a valid result. Here the source distribution is at a radius of 10λ and we are examining the fields in the vicinity of the caustic. It is also seen that the null position in this plot occurs at $x = \lambda/2$ again showing agreement with the previous statement that the caustic occupies the region $r/\lambda < 0.5$.

Conclusions

The caustic region on the back of a conducting cone for an axially incident electromagnetic wave is shown to extend to a distance on the order of $\lambda/2$ from the center of the caustic. This fixes the application of GTD analyses for cone back scatter to $ka > 3.0$. Such computations[8] have been made for cones as small as $ka = 2$ and reasonable results have been obtained. It may be possible to improve these results by replacing the 90° phase shift commonly caused by the caustic by the value given in Fig. 8 plus 45°. However, smaller cones could not be treated since the caustic would cover the entire base and the fields no longer have the local nature required by the ray optical or GTD analyses.

As has been noted earlier the results of this paper are applicable to finding the response of elemental antennas placed on the cone base, even for antennas mounted at the center of the caustic region. It is possible to consider smaller cones than the back scatter analysis, probably for base radii as small as $\lambda/4$, as fixed by the restriction on this distance of the observation point from the edge of the cone rim. Second order diffractions would again be in error but the fields from these rays would be small compared to the first order diffracted fields.

Similar comments may be made concerning the surface charge density induced on the cone base by an incident wave.

Appendix. Equations for "Acoustic Caustic" using Hard Boundary Condition

The pertinent caustic equations are presented here for the hard acoustic boundary condition.

Equation (8) becomes

$$I_\phi^h = \frac{j4}{k} G\left(n, \frac{3\pi}{2}\right) \tag{A-1}$$

Equation (9a) becomes

$$u = \frac{jka}{4\pi} \int_0^{2\pi} \frac{\left(\frac{j4}{k}\right) G\left(n, \frac{3\pi}{2}\right) e^{-jk|\bar{r}-\bar{r}'|}}{|r-r'|} \, d\phi' \tag{A-2}$$

Equation (13) becomes

$$u = A \int_0^{2\pi} e^{jkr\cos(\phi-\phi')}\, d\phi' \tag{A-3}$$

Equation (15) becomes

$$u = 2J_0(kr)\, G\left(n, \frac{3\pi}{2}\right) e^{-jk\left(a+\frac{r^2}{a}\right)} \tag{A-4}$$

Equation (A-4) differs significantly from Equation (15). The polarization factor ($\sin\phi'$) in Equation (13) caused the coefficient of the $J_0(kr)$ term to be zero for the electromagnetic case. If we retain the concept that the caustic region extends to the first null, then the "acoustic caustic" for the hard boundary condition extends only to $r < 0.4\lambda$ as compared to $r < 0.6\lambda$ for the electromagnetic caustic.

The form obtained for the restricted ranges of integration equivalent to Eq. (9b) is of limited merit in this case because of the severe discontinuity in the current density at $\phi' = 0, \pi$. This difficulty is averted in the electromagnetic case because of the presence of the $\sin\phi'$ factor in the integrand of Equation (9a).

It is worth noting that by use of the asymptotic form of $J_n(kr)$, both Equation (15) and Equation (A-4) can be obtained from the GTD analysis. To obtain Equation (A-4) for example, the expression for the GTD analysis is

$$u = u^i \sqrt{\frac{a}{r}} \left\{ 2v_B\left(n, a-r, \frac{3\pi}{2}\right) + 2v_B\left(n, a+r, \frac{3\pi}{2}\right) e^{j\frac{\pi}{2}} \right\}$$

and using the far field form of the diffraction coefficient yields

$$u = u^i \sqrt{\frac{a}{r}} \frac{2G\left(n, \frac{3\pi}{2}\right)}{\sqrt{2\pi ka}} \left\{ e^{-jk(a-r)}\, e^{-j\frac{\pi}{4}} + e^{-jk(a+r)}\, e^{-j\frac{\pi}{4}}\, e^{j\frac{\pi}{2}} \right\}$$

$$= u^i \frac{2G\left(n, \frac{3\pi}{2}\right)}{\sqrt{2\pi kr}} e^{-jka} \left[e^{j\left(kr-\frac{\pi}{4}\right)} + e^{-j\left(kr-\frac{\pi}{4}\right)} \right]$$

$$= u^i\, 2G\left(n, \frac{3\pi}{2}\right) e^{-jka} \sqrt{\frac{2}{\pi kr}} \cos\left(kr - \frac{\pi}{4}\right)$$

where $$J_0(kr) \sim \sqrt{\frac{2}{\pi kr}} \cos\left(kr - \frac{\pi}{4}\right)$$

References

1. Ryan, C.E., Jr., and Rudduck, R.C., "Calculation of the Far-Field Patterns of a Rectangular Waveguide," Report 1693-7, 20 November 1964, The Ohio State University ElectroScience Laboratory, Department of Electrical Engineering; prepared under Contract N62269-2184 for U. S. Naval Air Development Center. (AD 462 764).

2. Ryan, C.E. and Rudduck, R.C., "Radiation Patterns of Rectangular Waveguides," IEEE Trans. on Ant. and Prop., July 1968.

3. Ryan, C.E., Jr. and Peters, L., Jr., "Evaluation of Edge Diffracted Fields Including Equivalent Currents for the Caustic Regions," IEEE Trans. on Ant. and Prop., May 1969.

4. Ryan, C.E., Jr. and Peters, L., Jr., Correction to Evaluation of Edge Diffracted Fields Including Equivalent Currents for the Caustic Regions, IEEE Trans. on Ant. and Propagation, March 1970.

5. Ratnasiri, P.A.J., Kouyoumjian, R.G. and Pathak, P.H., "The Wide Angle Side Lobes of Reflector Antennas," Report 2183-1, March 1970, The Ohio State University ElectroScience Laboratory Department of Electrical Engineering; prepared under Contract AF 19(628)-5929 for Air Force Cambridge Research Labs.

6. Mentzer, C.A., Pathak, P.H. and Peters, L.,Jr., "Pattern Analysis of an Offset Fed Parabolic Reflector Antenna," Laboratory Report 3220-2, June 1972, The Ohio State University ElectroScience Laboratory Department of Electrical Engineering; prepared under Contract N00178-71-C-0264 for U. S. Naval Weapons Laboratory. (AFCRL-69-0413) (AD707105)

7. Senior, T.B.A. and Uslenghi, P.L.E., "High Frequency Back Scattering from a Finite Cone," Radio Science, March 1971.

8. Burnside, W.D. and Peters, L., Jr., "Axial Radar Cross Section of Finite Cones by Equivalent-Current Concept with Higher Order Diffraction," Radio Science, October 1972.

9. Hutchins, D.L. and Kouyoumjian, R.G., "A New Asymptotic Solution to the Diffraction by a Wedge," presented at 1967 URSI Meeting, Ottowa, Canada.

10. Harrington, R.F., "Time Harmonic Electromagnetic Fields," New York. McGraw-Hill, 1961, pp. 224, 237.

11. Collins, R.E., "Field Theory of Guided Wave," McGraw-Hill, 1960, p. 581.

12. Kay, I. and Keller, J.B., "Asymptotic Evaluation of the Field at a Caustic," J. Appl. Physics, July 1954.

13. Balanis, C.A., "Radiation from Conical Surfaces Used for High Speed Spacecraft," Radio Science, February 1972.

NASA-Langley, 1974 CR-2400